ELSEVIER

Physica C 272 (1996) 1–12

PHYSICA C

Texture analysis of Bi-2212 and 2223 tapes and wires by neutron diffraction

H.-R. Wenk [a,b,*], D. Chateigner [a,b], M. Pernet [b], J. Bingert [c], E. Hellstrom [d], B. Ouladdiaf [e]

[a] *Department of Geology and Geophysics, University of California, Berkeley CA 94720, USA*
[b] *Laboratoire Cristallographie-CNRS, BP 166, F-38042 Grenoble Cedex 9, France*
[c] *Center for Materials Science and MSTG-LANL, Los Alamos, NM 87545, USA*
[d] *Applied Superconductivity Center, University of Wisconsin, Madison, WI 53706-1687, USA*
[e] *ILL, BP 156, F-38042 Grenoble Cedex 9, France*

Received 4 September 1996

Abstract

The crystallographic texture of silver sheathed monocore tapes and wires, and multifilamentary tapes containing $Bi_2Sr_2CaCu_2O_x$ (Bi-2212) and $Bi_2Sr_2Ca_2Cu_3O_x$ (Bi-2223) superconducting oxides was determined by neutron diffraction, using a position sensitive detector. The orientation distribution (OD) was obtained from measurements of 4–6 pole figures. The oxide textures of these tapes and wires displayed axial symmetry, indicative of a grain-shape-controlled orientation mechanism. In monocore and multifilamentary tapes the *c*-axes of Bi-2212 and Bi-2223 are oriented perpendicular to the rolling plane, in wires they are perpendicular to the wire direction. The multifilamentary tape has the strongest texture with an OD maximum of 46 times that of a random sample. Monocore tapes are 26 and 35 mrd, and wires are 2.1 and 1.5 mrd. For comparison, a sinter-forged Bi-2223 barpowder was analyzed and exhibited *c*-axes parallel to the compression direction with a maximum of only 3.4 mrd. The texture of the silver sheaths depends on the processing conditions.

1. Introduction

Bismuth based high temperature superconductors are actually most amenable to the techniques currently available to manufacture long lengths of wire or tape with good performance, due particularly to their low weak link behavior compared to the yttrium or thallium based compounds. Even if their high magnetic field properties still require operating temperatures lower than liquid nitrogen, one can envisage 77 K applications in low or self-fields. Also, single crystals of $Bi_2Sr_2CaCu_2O_x$ (Bi-2212) and $Bi_2Sr_2Ca_2Cu_3O_x$ (Bi-2223) have a high shape anisotropy and occur as platelets and are amenable to various mechanical and thermal processing schemes to obtain high crystallite alignment. Since current transport is restricted to the {001} (basal) plane, high alignment (texture) is essential to obtain large critical currents, as has been documented by various studies [1,2]. Whereas the importance of texturing is generally recognized, and manufacturing methods have been improved to produce a high degree of crystallite alignment [3–5], there is very little quantitative information about the actual textures of Bi-2212 and

* Corresponding author. Fax: +1 510 643 9980; e-mail: wenk@eismo.berkeley, edw.

PII S0921-4534(96)00561-8

Bi-2223 tapes and wires. This has various reasons. Samples are generally small and fairly heterogeneous, not providing enough homogeneous surface for quantitative X-ray examination. Diffraction patterns are complex with many overlapping diffraction peaks which are difficult to resolve with a conventional X-ray pole figure goniometer. The Bi-2212 samples have often what appears to be a poor crystallinity with a small peak to background ratio. We have chosen neutron diffraction to overcome some of these limitations [6,7] and are reporting texture results on various tapes and wires, fabricated by different processes in several laboratories.

Different methods have been used in the past to obtain texturing. Techniques using axial stress produce a low degree of crystallite orientation [8,9], even in conjunction with a high magnetic field [10], and correspondingly low critical current densities. The so-called MTG (melt textured growth) technique which appears promising because it produces reasonable physical properties in the Y–Ba–Cu–O system [11] is not suitable for Bi-2212 and Bi-2223 compounds because of the greater complexity of their phase diagram. Superconductor compounds are sheathed in silver, fabricated into a tape or wire using wire manufacturing techniques, then thermally treated to produce a practical superconductor that is more adapted for embedding in silver sheaths and consecutive cold or hot deformation and thermal treatment [12]. Silver is used as the sheath material due to its chemical compatibility with Bi-2212 and Bi-2223, desired phase development requirements during sintering, and oxygen diffusivity and oxidation resistance at elevated temperature. Silver supplies ductility and protection for the tape or wire for use in potential applications such as long power transmission lines and superconducting coils. Oxide textures can be very strong and high J_c have been obtained [13]. Multifilamentary conductors are advantageous since the current is shared by multiple parallel conducting paths [14,15].

2. Samples

Samples of Bi-2212 and Bi-2223 tapes and wires were obtained from three different laboratories (Table 1). Ideally one would like to use texture analysis to quantitatively relate preferred orientation to physical properties, or at least to manufacturing conditions. Unfortunately, the physical properties of the samples used for this study were not well characterized. We assume that they resemble comparative samples that have been described in the literature.

The general procedure to manufacture wires and tapes [3,16] is termed the "oxide powder in tube" method (OPIT). A fine powder of Bi-2212 or Bi-2223 is filled into a silver tube (e.g. 10 cm long and 1 cm in diameter). The tube is then drawn to a wire in many passes, obtaining about a 70% packing density of the oxide powder. The wire can then be thermally processed as-is. It can also be rolled to a flat tape, or a multifilament tape may be prepared by bundling several wires, encasing them in another silver tube, redrawing, and rolling. Usually this mechanical processing is performed at room temperature but hot rolling has also been used [17]. To complete the oxide phase reaction and connect the grains in the wire or tape, the tapes need to be thermally treated. Controlling the time, temperature, and atmosphere lead to closed grain boundaries and optimal oxygen stoichiometry [15,18].

Table 1
Quantitative characterization of Bi samples

Sample #	Description	Counting time (s)	2θ (°) FWHM	RP (%)	F^2	ODF (mrd)		{001} max (mrd)	$\{001\}_{WHM}$ (°)	RD max (mrd)
						min	max			
T 2212	Tape	600	0.34	11.4	11.06	0	32.6	26.2	21	4.2
MF 2212	Multifilament	900	0.65	9.1	17.59	0	46.0	46.0	17	5.7
T 2223	Tape	600	0.41	4.6	11.11	0	32.3	34.6	19	5
W-W 2212	Wire	1600	0.48	8.1	1.50	0.1	3.6	2.1	34	–
W-LA 2212	Wire	1200	0.82	3.5	1.20	0.1	1.6	1.5	66	–
P 2223	Powder	400	0.37	2.5	1.44	0.5	3.4	3.3	50	1.5

The Bi-2212 monocore tape and wire, and the multifilamentary tape from the University of Wisconsin (T-2212, W-W 2212, MF 2212) were produced by drawing and rolling as described above. Afterwards they were melt processed in 100% O_2 [14,15]. This produces practically a single phase Bi-2212 microstructure, and J_c values up to 100–200 kA cm^{-2} (4 K, 0 T) have been measured in tapes produced similarly [19].

The Bi-2212 wire from Los Alamos (W-LA 2212) was fabricated using the standard OPIT method [3]. The 2212 powder was obtained from Seattle Speciality Ceramics, and was vacuum calcined to remove the majority of carbon in the as-received powder. This powder was packed into a 1.27 cm silver tube that was drawn in multiple passes to a 1 mm diameter wire, all at room temperature. The wire used for the neutron diffraction studies was in the as-drawn condition and had received no thermal processing, so it did not carry supercurrent.

The Bi-2223 tape from the University of Geneva (T 2223) is allegedly a pressed and cold-rolled tape material that has been described previously [20]. In those samples, the calcined precursor powder consisted mainly of Bi-2212. It was packed into 8 mm diameter silver tubes, drawn to 1 mm diameter wires and then rolled to a tape with 0.1 mm thickness and 3 mm wide. The oxide core represents about 30% of the total cross section. The Bi-2212 tapes were then heat treated at 840°C in air to form Bi-2223. The cold-rolled tapes exhibit J_c of 18 500 A cm^{-2} (77 K and 0 T) and 3550 A cm^{-2} (77 K and 3 T).

A sinter-forged hot-pressed Bi bar of 2223 powder produced at Argonne (P 2223) was studied for comparison to the tapes and wires. The 84–95% dense (Bi,Pb)SrCaCuO bars were fabricated by sinter-forging at 850°C [21]. These samples exhibit transport critical current densities of 8×10^3 A cm^{-2} at 77 K in a self-field.

3. Diffraction experimental procedures and data analysis

In all the tapes and wires, the superconducting oxide phase was sheathed in silver, and when Ag was present in the neutron diffraction samples, it dominated the diffraction pattern. Where possible, an attempt was made to concentrate the oxide by removing as much silver as possible by etching. The tapes and wires were then cut into segments ranging from 5 to 10 mm long, and these segments were glued together to form a cube, keeping the segments strictly parallel (Fig. 1). An effort was made to minimize the amount of glue that was used to avoid diffuse scattering of neutrons by hydrogen.

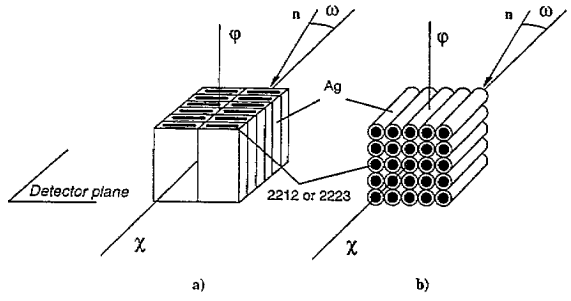

Fig. 1. Typical tape (a) and wire (b) samples used for neutron diffraction experiments. Definition of the rotations φ, χ and ω used in this study for the pole figure scans. Samples are positioned with their symmetry axis perpendicular to the φ circle. n indicates the direction of the incident neutron beam..

Most texture measurements were done at the high flux neutron source of the Institut Max von Laue–Paul Langevin (ILL) at Grenoble, France, using the instrument D1B and following procedures similar to those described previously [7]. The radiation applied was a monochromated beam of neutrons with a wavelength of 2.523 Å and a flux at the sample of 6×10^6 neutrons cm^{-2} s^{-1}. The sample was mounted on an Eulerian cradle and could be brought into any arbitrary orientation by rotations about two axes, χ and φ (Fig. 1). Diffractometer coordinates χ, φ are converted to pole figure coordinates α, β which depend on the setting of the Eulerian cradle angle (ω) and the Bragg angle (2θ) [22]. Diffracted intensities are recorded with a position sensitive detector composed of 400 cells which span a 2θ range of 80°. Depending on the sample size, and particularly the volume of superconductor in the sample, different recording times were required, ranging from 400 s for a 10 mm cube from the sinter-forged hot-pressed powder to 1600 s for a 5 mm cube of Ag-sheathed wire with silver attached (Table 1). In the latter case the time was just long

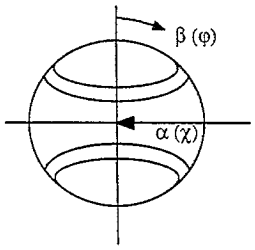

Fig. 2. Pole figure of an axisymmetric texture with pole figure coordinates α, β and diffractometer coordinates χ, φ. Also indicated are scans to establish axial symmetry (α) and to determine the texture (β).

enough to be at the limit of satisfactory counting statistics.

Wires have axially symmetric textures due to the production process. Therefore it is not necessary to measure a complete pole figure; one only needs to take a profile at angles ranging from parallel to perpendicular to the wire axis. This was done with a φ-scan to avoid complications with a blind area in the center of the pole figure (Fig. 2). For tapes axial symmetry about the rolling plane normal needed to be established first which was done with a χ-scan. Fig. 3 shows spectra for different χ angles for the monocore and multifilamentary Bi-2212 tapes illustrated in Fig. 1. For the monocore tape T 2212 (Fig. 3(a)) all five spectra are very similar, which establishes, for all practical purposes, axial symmetry.

For the multifilamentary tape MF 2212 (Fig. 3(b)) there are intensity changes for Ag when the sample is rotated about χ. This can be expected due to the formation of typical non-axisymmetric rolling textures in cubic metals. There are also minor intensity variations for Bi-2212, particularly noticeable for the 200 peak. This could be due to an "in-plane" orientation of a-axes in this sample.

In such a case a complete pole figure is necessary to characterize the texture. Unfortunately, there was not sufficient time left at ILL to measure a complete pole figure. Several months later we had the opportunity to measure the same sample at the Laboratoire Léon Brillouin (LLB) in Saclay, France, with monochromatic neutrons ($\lambda = 1.158$ Å) and a point detector. This diffractometer is mainly used for metals and the collimation geometry produces a very high background for weakly scattering materials. Due to some geometrical effect of sample, the horizontal plane of all pole figures, including silver, was slightly undersampled (Fig. 4). In spite of both this effect and poor counting statistics, we could establish that pole figures of Bi-2212 are indeed axially symmetric (Fig. 4(a)) and that the apparent deviations in Fig. 3(b) can be attributed to a slight displacement of the symmetry axis relative to the goniometer frame. The ILL data with only χ-scans were therefore sufficient to determine the textures quantitatively.

All axisymmetric textures can be characterized by profiles taken over angular ranges from (1) normal to parallel to the tape surface, and (2) normal to perpendicular to the wire direction. These profiles are conveniently measured at ILL D1B in a φ-scan. The φ-scans extended over a range of 180° to ascertain homogeneity and were done in increments of 5°. Later, during data processing, the 180° sector was reduced to a 90° sector by averaging.

Fig. 5 shows averages of all diffraction spectra measured with a position sensitive detector for all

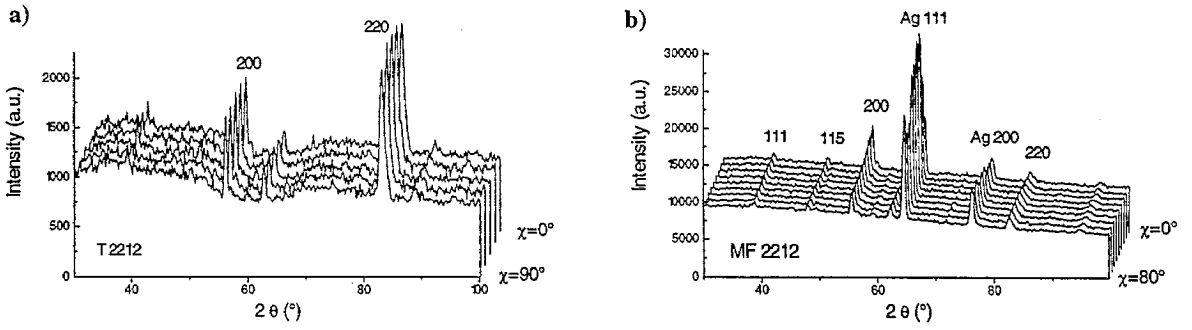

Fig. 3. 2θ spectra at different χ positions (α-scans in Fig. 2), documenting the axisymmetry of the texture. (a) Tape T 2212 with silver removed. (b) Apparent partial in-plane alignment for the Bi 2212 multifilament particularly visible for (200) which is due to a slight sample misalignment and for silver due to a non-axial texture with strong in-plane alignment.

the measured samples. In these, texture effects are partially removed. The patterns help illustrate the difficulties with these measurements. Particularly in the Bi-2212 oxides, the apparent crystallinity is poor with many of the peaks being barely above the high and varying background. In the samples T 2212 and W-W 2212 (Figs. 5(a), 5(d)) there is a variation in background with diffraction angle that may be due to the presence of adhesive medium. Another possible source of the continuous scattering may be from the quartz-glass sample holder. However, the same sample holder was also used for tape T 2223 where the

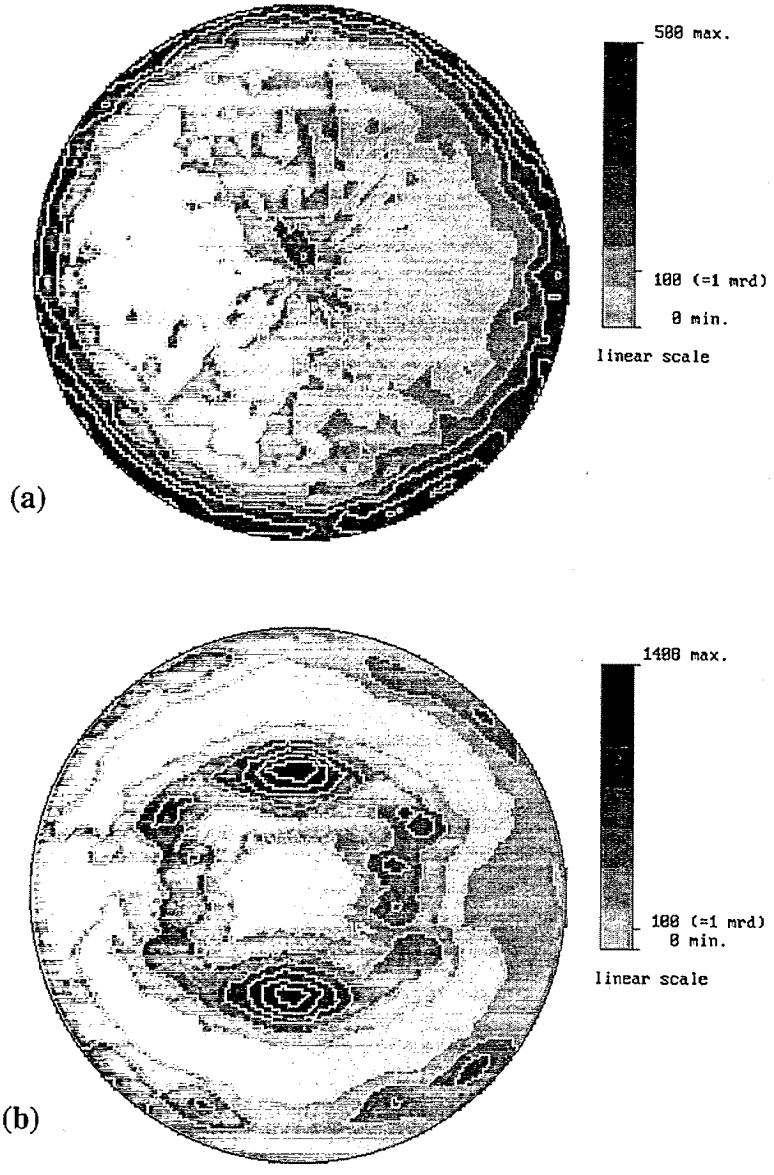

Fig. 4. Complete pole figures of multifilament MF 2212 measured by neutron diffraction at LLB. (a) {220} reflection of Bi-2212. The small concentration in the center is due to a contribution from the superposed reflection {0016}, (b) {111} reflection of silver. Equal area projection.

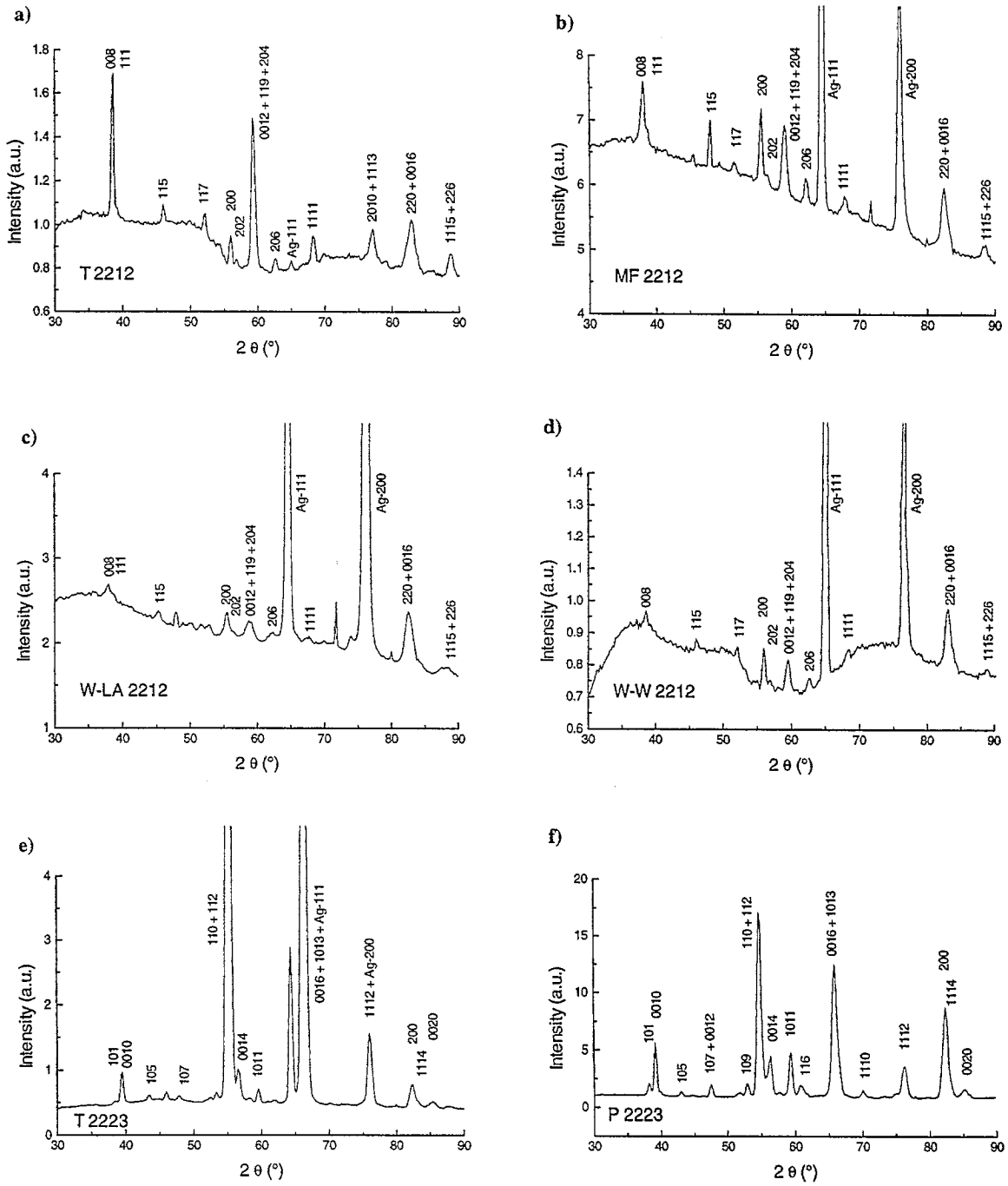

Fig. 5. Sum of all diffraction spectra for each sample, illustrating resolution and statistics. For T 2212, silver has been removed. Diffraction indices are assigned to most discernable peaks. Scales are different and have different origins.

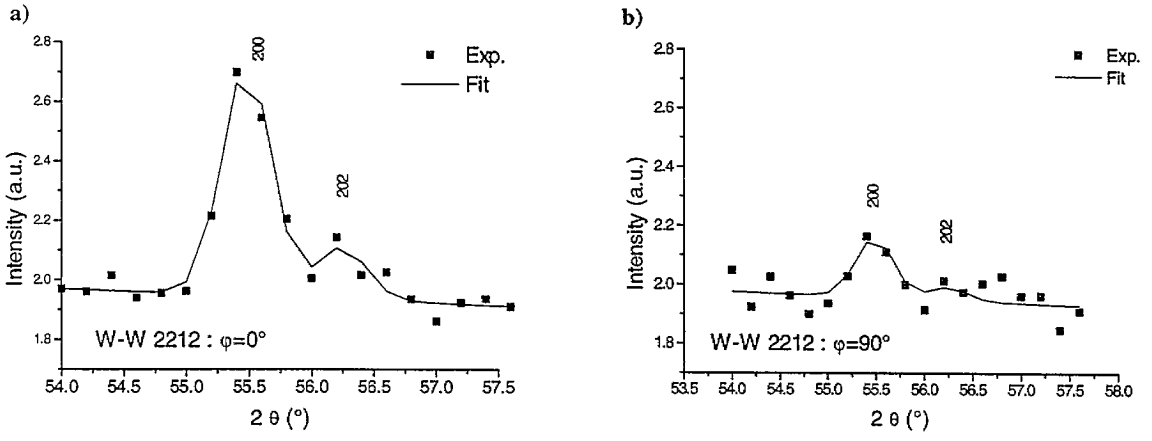

Fig. 6. Result of the fit of the 200 and 202 reflections with Gaussians for two sample orientations of the wire W-W 2212; (a) is in a texture maximum, (b) in a texture minimum.

background was much lower and fairly constant. In the Bi-2212 wire W-LA 2212 (Fig. 5(c)), the diffraction intensities are very low and peak widths are large. The low diffraction intensities and large peak widths observed for this sample may be associated with its "as-drawn" condition. Deformation-induced loss of crystallinity is a common feature in Bi-2212. In the Bi-2223 samples, the oxide's crystallinity is generally better as seen in Table 1, which gives a comparison of the full widths at half maximum (FWHM) of a Bragg peak located at similar angles for Bi-2212 and Bi-2223 phases (008 and 0010 respectively). Clearly the wire W-LA 2212 has the largest peak width. This variation in peak width was not analyzed in detail since it depends on many factors such as crystallinity, sample size, and the collimation system. In comparison, the Ag peak FWHM for the Ag 111 reflection ranges between 0.4° and 0.53°, which is significantly smaller (noticeably lower than for W-LA or MF Bi-2212 oxide). For the Bi-2223 tape the tendency is reversed with 0.67° FWHM of the Ag 111 peak, a sign of a greater deformation of silver in this sample. As mentioned earlier, whenever silver is present, it dominates the diffraction pattern, as seen in Fig. 5. Some peaks are indexed in the diffraction patterns, based

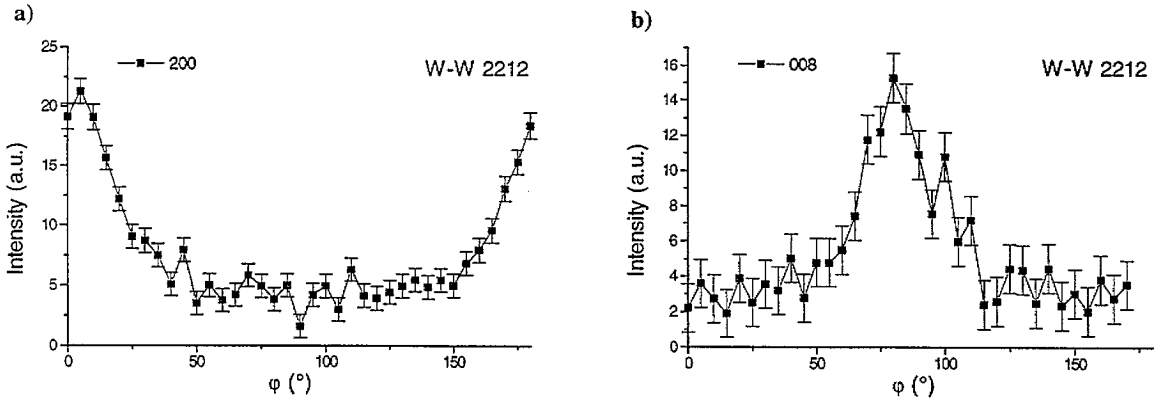

Fig. 7. Results of a φ-scan for the wire W-W 2212 illustrating texture intensities for (a) (008) and (b) (200) as function of φ. Based on such profiles the orientation distribution was calculated. Bars are one standard deviation.

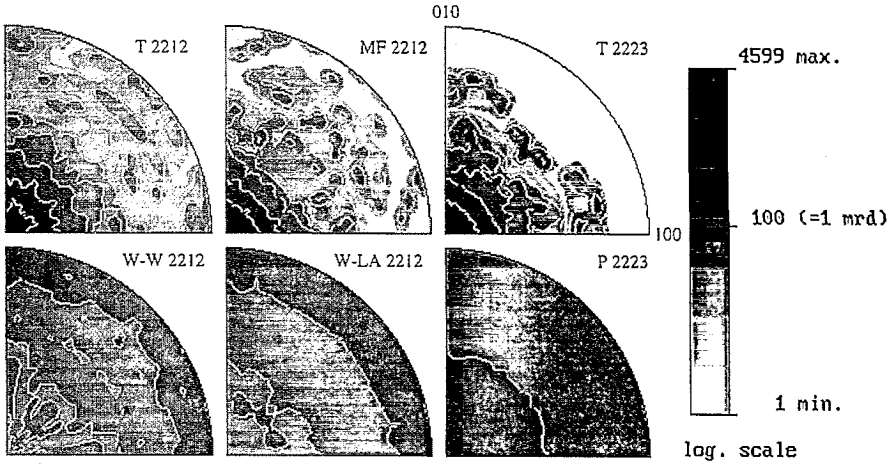

Fig. 8. Inverse pole figures for the six analyzed Bi-2212 and Bi-2223 samples. For tapes inverse pole figures are for the normal to the rolling plane, for wires for the wire direction and for the pressed powder for the compression direction. Equal area projection. Units are in mrd.

on the known crystal structures [23]. There are some peaks, particularly in the T 2223 tape, that could not be identified and must be due to the presence of non-superconducting phases.

Various methods have been used to extract intensity information from the diffraction pattern, including the Rietveld method [24]. In our study, pattern matching was not successful, largely because of the

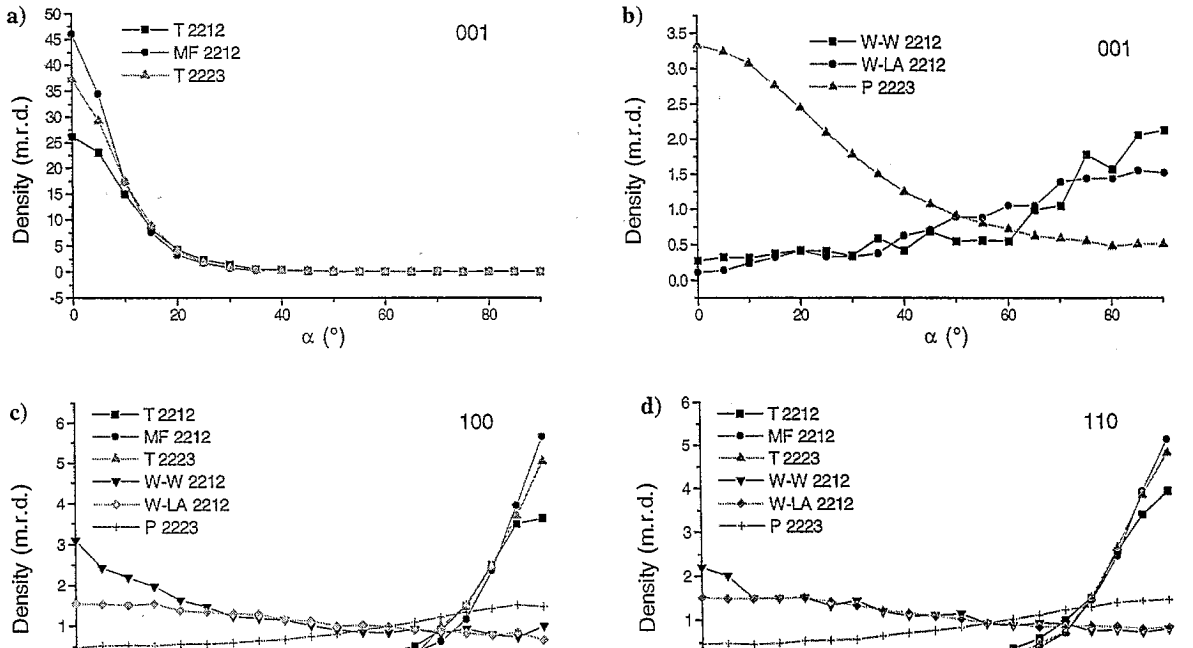

Fig. 9. Recalculated Bi-2212 and Bi-2223 (001), (100) and (110) texture profiles for the six analyzed samples. Profiles extend from parallel to the symmetry axis ($\alpha = 0°$) to perpendicular to the symmetry axis ($\alpha = 90°$).

high and irregular background. After various trials we applied the same method which we used previously [7], i.e. to fit individual peaks with Gaussians (program XRFIT, [25,26]). At first the peak positions and peak widths of reflections were refined on the average spectra of Fig. 5. Then positions and widths were kept constant and the peak intensities only were refined on individual spectra. Background was obtained at two fixed angular positions and the average refined value was subtracted. The Gaussian fit provides a net intensity and standard deviation. Fig. 6 illustrates the fit of the overlapping 200/202 peaks of W-W 2212 at a sample orientation that shows a texture maximum (Fig. 6(a)) and another that shows a minimum (Fig. 6(b)). This demonstrates some of the problems introduced by counting statistics. Due to the high overall background relative to the peak intensities and due to the strong textures, standard deviations are high and often similar to net intensities in the texture minima. Depending on the background count in a particular spectrum, net intensities in these low orientation density regions were occasionally negative. Calculated negative intensities were set to zero.

Fig. 7 displays integrated intensity variations for the W-W 2212 wire data of the weak 008 reflection and the stronger 200 reflection from W-W 2212 as a function of φ. The standard deviation is indicated. These data were averaged into a 90° sector and values from 3 or 4 different *hkl* peaks were used to calculate the orientation distribution (OD) using the WIMV method [27] in the software package BEARTEX [28]. For lack of detailed diffraction data, tetragonal crystal symmetry had to be assumed. For Bi-2212 only 4 peaks (008, 117, 200 and 220) showed sufficient counting statistics and lack of overlap with other Bi-2212 peaks or diffraction peaks from other phases to provide useful information. Consideration was given to the fact that the measured 220 reflection is actually a composite of 220 (98%), 0016 (1.5%) and 202 (0.5%). For the Bi-2223 tape 101, 0010 and 1011 reflections were used. Due to the 2θ proximity of 101 and 0010, only the $60° < \alpha < 90°$ region of the 101 pole figure was used to calculate the OD.

From the ODF, inverse pole figures were calculated (Fig. 8) representing the density distribution of the symmetry axis (tape normal and wire direction, respectively) relative to the crystal coordinates. Also, 001, 100 and 110 pole figures were recalculated and are represented in Fig. 9 as profiles due to the imposed axial symmetry.

4. Results

All the tape samples that were measured showed strong textures with *c*-axis maxima up to 46 mrd, i.e. an alignment which is up to 46 times stronger than in a sample with a uniform (random) orientation distribution. This is visible in the inverse pole figures, which are a compact representation of axially symmetric textures (Fig. 8). For tapes these display a maximum at (001). The (001) pole profiles (Figs. 9(a), 9(b)) have a nearly Gaussian shape with widths (FWHM) ranging from 17° (MF 2212) to 21° (T 2212), which is comparable to data in the literature [29]. Besides angular widths of diffraction and texture peaks, Table 1 summarizes other texture information such as maxima and minima in the OD, 001 pole figure maxima, texture index F^2, which is a measure of the overall texture strength [30], and RP values for the maximal regions above 1 mrd (these latter are a measure for the quality of the ODF refinement; the higher the RP values, the lower is the quality of the refinement). The RP values depend on the overall texture strength and we found them to be in a satisfactory range.

For the wires, the wire direction inverse pole figures display a maximum region consisting of a girdle at high angles to (001) extending from (100) to (110). There does not appear to be any significant preference for (100) or (110) but information on this is limited by the experimental data. The (100) and (110) profiles are very similar (Figs. 9(c), 9(d)). For the wires the (001) densities are much lower than for the tapes because the *c*-axes form a girdle distribution, rather than a single maximum. It is interesting that the thermally treated wire W-W 2212 and the cold-drawn wire W-LA 2212 have a very similar texture, indicating that the texture pattern becomes established during the deformation process rather than the heat treatment.

The wire texture can be compared with a tape texture that has been symmetrically averaged around the rolling direction (RD). This corresponds to an

inverse pole figure for the rolling direction. We have calculated such RD inverse pole figures of our tape and powder samples. The last column in Table 1 gives the maximal densities (right column) along the rolling direction for tapes and perpendicular to the pressure axis for the powder. Interestingly all the tapes possess significantly higher densities than the one measured for wires. Thus the level of orientation in wires does not achieve current transport capabilities as high as in tapes.

In samples with silver present we also measured its texture. The Ag {111} pole figure for the multifilament tape MF 2212 (measured at LLB) displays a typical rolling texture (Fig. 4(b)). We calculated the Ag inverse pole figure of wires from the {111} and {200} intensity profiles. In as-drawn wire W-LA 2212 a strong 001 component (16 mrd) and a weaker 111 component (2.2 mrd) are observed in the inverse pole figure (Fig. 10(a)). This is typical of silver, which possesses a low stacking fault energy, while most other f.c.c. metals have a stronger ⟨111⟩ component. Ahlborn and Wassermann [31] described a 99.99% Ag wire with a ⟨001⟩/⟨111⟩ ratio of 1.2, which is significantly lower than the 7.5% ratio that we observed in sample W-LA 2212. However, the ⟨001⟩/⟨111⟩ ratio reportedly increases with continued deformation [32] and recrystallization [33]. Since the wire in this study underwent a strain of > -5, and since high purity Ag probably statically recrystallizes at room temperature after such large strains, the high ratio is reasonably consistent. The wire W-W 2212, processed at the Wisconsin laboratory shows a rather complicated texture with a maximum near ⟨102⟩ of 2.7 mrd (Fig. 10(b)). It probably formed during the thermal treatment. It is rather surprising that the silver texture in the cold-rolled Bi 2223 tape T 2223 produced in Geneva is close to random with no regular pattern. This may have occurred due to exaggerated grain growth during the postrolling thermal treatment as the Bi-2212 was transformed to Bi-2223. All the silver had been removed from T 2212.

It has been pointed out above that all the oxide textures in the bismuth tapes, are axially symmetric (fiber textures). This is a strong indication that the crystallite alignment in these materials is due to the platy shape of the particles [8,34] and subsequent growth, rather than due to intracrystalline slip processes [35] where one would expect to see some difference between (100) and (110) during rolling, resulting in a preferred directional alignment of a and b axes within the plane of the tape. We attribute deviations from axial symmetry in previously reported pole figures measured by X-ray diffraction to artifacts of the measuring technique, with the X-ray beam leaving part of the sample in certain orientations [34]. One of the advantages of using neutron diffraction is that the whole volume of the sample remains immersed in the neutron beam at all orientations. This is particularly critical for the multifilament sample which is practically impossible to study by conventional X-ray techniques.

For comparison we have also measured the texture of P 2223, a sinter-forged hot-pressed bar of

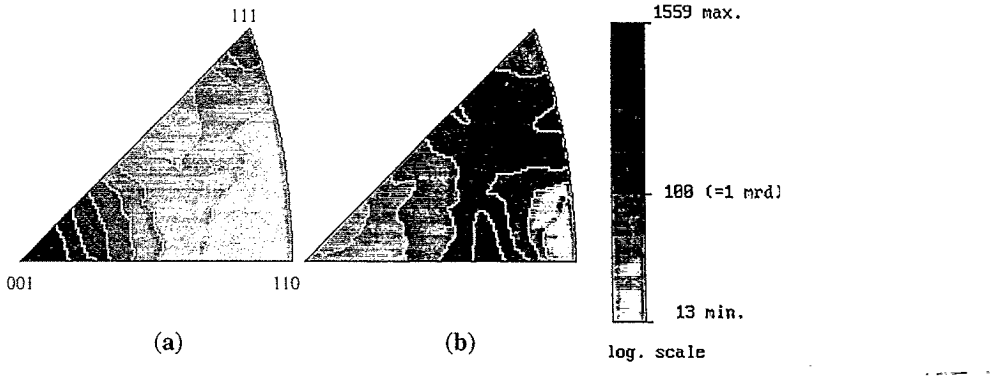

Fig. 10. Inverse pole figures of the wire direction for silver in wires. (a) Cold deformed wire W-LA 2212, "as-received", (b) annealed wire W-W 2212. Equal area projection. Units are in mrd.

bulk Bi 2223 powder. The measured texture (3.43 mrd) is much weaker in strength than the texture in tape T 2223, but similar in pattern with a 001 maximum in the compression direction (Fig. 9(b)). The strength of the texture is comparable to that of cold-pressed Bi 2223 powders [8]. Again in P 2223 there are no deviations from axial symmetry, which argues against intracrystalline plasticity. The neutron texture measured at ILL is similar to that determined by X-ray techniques [21].

5. Conclusions

In this study we found that neutron diffraction is a suitable method to characterize quantitatively the textures of Bi-2212 and 2223 wires and tapes, even if the material appears to have poor crystallinity and diffraction patterns have a small peak to background ratio. This lack of crystallinity often made the measurements and data reduction difficult and one had to work at the limit of resolution due to peak overlaps and poor counting statistics.

The observed textures in the Bi-2212 and Bi-2223 tapes are extremely strong. It indicates that manufacturing techniques have become very efficient in texturing for materials with anisotropic grain shapes and can produce homogeneous textures at the meter scale or more. Achieving strong texturing requires that the volume of non-superconducting second phases is minimal.

A comparison of textures in as-drawn and annealed Bi-2212 wires suggests the final texture is established during deformation processing, then is sharpened but otherwise unaltered during sintering. The deformation texture would seem to provide a template for grain growth. Additional experimentation is required to ascertain if this association holds for tapes and for Bi-2223, and whether a direct relationship exists between texture sharpness and transport properties.

Acknowledgements

We acknowledge G. Grasso and R. Flukiger of the University of Geneva and L. Motowidlo of Inc. IGC Advanced Superconductors, for providing some samples. We thank M. Mathon and R. Penelle from LLB, Saclay, and F. Brunet from the Laboratoire Cristallographie-CNRS, Grenoble for giving access and help during experiments at LLB. The ILL and LLB research facilities were crucial for performing this research. H.R.W. appreciates support from NSF grant EAR 94-17580 for texture research and hospitality at the Laboratoire Cristallographie, Grenoble during a sabbatical leave.

References

[1] S. Jin, T.H. Tiefel, R. Sherwood, M. Davis, R. van Dover, G. Kammlott, R. Fastnacht and H. Keith, Appl. Phys. Lett. 52 (1988) 2074.
[2] D. Dimos and P. Chaudhari, Phys. Rev. Lett. 61 (1988) 219.
[3] K.H. Sandhage Jr., G.N. Riley and W.L. Carter, J. Met. 43 (1991) 21.
[4] W. Lo and B. Glowacki, Supercond. Sci. Technol. 4 (1991) S361.
[5] J. Yoo and K. Mukherjee, Physica C 222 (1994) 241.
[6] M. Okada, A. Okayama, T. Matsumoto, K. Aihara, S. Matsuda, K. Ozawa, Y. Morii and S. Funahashi, Jpn. J. Appl. Phys. 27 (1988) L1715.
[7] H.R. Wenk, J. Pannetier, G. Bussod and A. Pechenik, J. Appl. Phys. 65 (1989) 4070.
[8] M. Sintubin, H.-R. Wenk and D.S. Phillips, Mater. Sci. Eng. A 202 (1995) 157.
[9] V. Plechacek, H. Hejdova and Z. Trejbalova, Cryogenics 30 (1990) 750.
[10] J.G. Noudem, J. Beille, E. Beaugnon, D. Bourgault, D. Chateigner, P. Germi, M. Pernet, A. Sulpice and R. Tournier, Supercond. Sci. Technol. 8 (1995) 558.
[11] P. de Rango, M. Lees, P. Lejay, A. Sulpice, R. Tournier, M. Ingold, P. Germi and M. Pernet, Nature 349 (1991) 770.
[12] P. Haldar, J. Hoehn, J. Rice and L. Motowidlo, Appl. Phys. Lett. 60 (1992) 495.
[13] G. Grasso, B. Hensel, A. Jeremie and R. Flukiger, Physica C 241 (1995) 45.
[14] E.E. Hellstrom, in: High-Temperature Superconducting Materials Science and Engineering: New Concepts and Technology, ed. D.L. Shi (Pergamon, 1995) p. 383.
[15] L.R. Motowidlo, G. Galinski, G. Ozeryansky, W. Zhang, and E.E. Hellstrom, Appl. Phys. Lett. 65 (1994) 2731.
[16] R. Flukiger, B. Hensel, A. Jeremie, A. Perin and J. Grivel, Appl. Supercond. 1 (1993) 709.
[17] A. Perin, G. Grasso, M. Daumling, B. Hensel, F. Walker and R. Flukiger, Physica C 216 (1993) 339.
[18] W. Zhang and E.E. Hellstrom, Supercond. Sci. Technol. 8 (1995) 430.
[19] W. Zhang, E.A. Goodilin and E.E. Hellstrom, Supercond. Sci. Technol. 9 (1996) 211.
[20] G. Grasso, A. Perin, B. Hensel and R. Flukiger, Physica C 217 (1993) 335.

[21] N. Chen, A.C. Biondo, S.E. Dorris, K.C. Goretta, M.T. Lanagan, C.A. Youngdahl and R.B. Poeppel, Supercond. Sci. Technol. 6 (1993) 674.
[22] H.J. Bunge, H.R. Wenk and J. Pannetier, Text. Microstruct. 5 (1982) 153.
[23] D.P. Matheis and R.L. Snyder, Powder Diffract. 5 (1990) 8.
[24] L. Lutterotti, S. Matthies and H.-R. Wenk, J. Appl. Phys. (1996), in press.
[25] J. Rodriguez, M. Anne and J. Pannetier, 1987 STRAP, A System for Time-Resolved Data Analysis (Powder Diffraction Patterns), ILL Grenoble Internal Rep. 87 RO14T.
[26] A. Filhol, H.Y. Blanc, A. Antoniadis and J. Berruyer, ILL Grenoble Internal Rep. 88 FI05T.
[27] Matthies and Vinel, Phys. Stat. Sol. B 112 (1982) K111.
[28] H.R. Wenk, S. Matthies and J. Donovan, Textures of Materials, ICOTOM 11 (Int. Acad. Publ., Beijing, 1996) p. 212.
[29] D. Schlaefer, K. Fischer, M. Schubert and B. Schlobach, Text. Microstruct. 24 (1995) 93.
[30] H.J. Bunge, Texture Analysis in Materials Science (Butterworths, London, 1982).
[31] H. Ahlborn and G. Wassermann, Z. Metallkd. 53 (1962) 422.
[32] I.L. Dillamore and W.T. Roberts, Metall. Rev. 10 (1965) 330.
[33] M. Wilhelm, B. Roas, H. Helldorfer and A. Jenovelis, Proc. ISS 93 (1993), Hiroshima, p. 26.
[34] H.R. Wenk and D.S. Phillips, Physica C 200 (1992) 105.
[35] R.J. Asaro, S. Ahzi, W. Blumenthal and A. DiGiovanni, Phil. Mag. A 66 (1992) 517.